Scale Size of Magnetic Turbulence in Tokamaks Probed with 30-MeV Electrons

I. Entrop,[1] N. J. Lopes Cardozo,[1] R. Jaspers,[1] and K. H. Finken[2]

(Partners in Trilateral Euregio Cluster)

[1]*FOM-Instituut voor Plasmafysica "Rijnhuizen," Association Euratom-FOM, P.O. Box 1207, 3430 BE Nieuwegein, The Netherlands*
[2]*Institut für Plasmaphysik, Forschungszentrum Jülich GmbH, EURATOM Association, D-52425 Jülich, Germany*

Measurements of synchrotron radiation emitted by 30-MeV runaway electrons in the TEXTOR-94 tokamak show that the runaway population decays after switching on neutral beam injection (NBI). The decay starts only with a significant delay, which decreases with increasing NBI heating power. This delay provides direct evidence of the energy dependence of runaway confinement, which is expected if magnetic modes govern the loss of runaways. Application of the theory by Mynick and Strachan [Phys. Fluids **24**, 695 (1981)] yields estimates for the "mode width" (δ) of magnetic perturbations: $\delta < 0.5$ cm in Ohmic discharges, increasing to $\delta = 4.4$ cm for 0.6 MW NBI.

PACS numbers: 52.55.Fa

One of the outstanding issues in thermonuclear fusion research remains the anomalous conduction of heat by the electrons in the plasma. In a tokamak, the hot plasma is confined in a toroidal geometry by means of magnetic fields. The field topology is such that field lines lie on nested toroidal surfaces. Transport in the direction perpendicular to the surfaces is reduced by many orders of magnitude by the presence of the field. However, the measured heat fluxes carried by the electrons exceed the theoretically achievable minimum by 1–2 orders of magnitude. This anomaly is generally ascribed to turbulence, which may be of electrostatic or of magnetic nature, or both. There has been extensive research into transport caused by electrostatic fluctuations. Recently, means have been found to greatly reduce the heat loss caused by these [1]. Magnetic turbulence is more difficult to diagnose, since perturbing fields of the order $\tilde{B}/B = 10^{-5}$ can already contribute significantly to the heat flux carried by the electrons. The only direct measurements of $\tilde{B}$ in the core of a tokamak plasma, using the cross-polarization scattering of microwaves, did show the presence of $\tilde{B}$ at transport relevant levels in Tore Supra [2,3].

Electrons with energy much higher than the thermal energy, in principle, can provide a probe to study magnetic turbulence, since diffusion due to electrostatic turbulence scales with v^{-1}, whereas the magnetically induced diffusion scales as v, where v is the electron velocity. Moreover, since in a plasma the mean free path of an electron scales as v^4, collisional transport is negligibly small for high energy electrons. The absence of collisions is also the reason why in tokamak plasmas of sufficiently low density a small fraction of the electrons (so-called runaway electrons) undergo a free fall acceleration and can reach energies in the MeV range, in a background plasma with a temperature of ~1 keV.

In several studies, runaway electrons have been used to assess magnetic turbulence. One principal difficulty is

that runaway electrons in the 1-MeV energy range cannot be diagnosed until they leave the plasma and hit the wall and produce x rays. Thus, in [4] experimental techniques have been used to probe magnetic turbulence in the edge of the plasma. Direct observation of runaway electrons in the center of the plasma column has been performed at the TEXTOR-94 experiment, making use of the synchrotron emission. This method diagnoses runaway electrons in a much higher energy range, typically 25–30 MeV. The high energy poses another problem. The orbits of electrons of such high energy are shifted with respect to the magnetic field topology by a few cm, which strongly reduces their sensitivity to magnetic perturbations with a radial correlation length smaller than this orbit shift [5]. In fact, this orbit shift is the reason why high energy runaway electrons are often observed to have much better confinement than then thermal electrons (e.g., [6,7]).

So, the question is, How can the observable high energy runaway electrons be used to probe magnetic turbulence with a scale much smaller than their orbit shift?

In this Letter, an analysis is presented based on a novel observation: when auxiliary heating is applied to a plasma with a preexisting runaway population, this population is observed to decrease. Clearly, the runaway confinement is deteriorated by the power input, which is expected since it is well known that confinement of heat and thermal particles also degrades with increasing heating power. However, the decline of the runaway population does not start instantaneously after the heating is switched on, but is significantly delayed. It is shown that this delay is due to loss of runaway confinement at a lower energy, which only later appears as reduced influx of observable runaway electrons at high energy. In this picture, there is a certain energy below which the runaway electrons are lost. The delay time in the radiation signals is the time the electrons at this energy need to be accelerated to the energy where they become observable. Thus, the delay time can be related to a

loss energy W_{loss}, and so to the radial scale length of the magnetic turbulence.

In [5] the energy dependence of runaway confinement, based on the averaging effect of the orbit shift, is calculated and related to the "mode width" δ of the magnetic perturbations. This theory has been applied to the present data to refine the estimate of the radial scale length of the magnetic perturbations. Since the delay depends on the level of neutral beam injection (NBI), so does δ. Thus, from the dynamic evolution after NBI switch-on of a runaway population at 30 MeV, conclusions can be drawn on the grain size of magnetic turbulence as a function of NBI power.

The experiments were carried out in the TEXTOR-94 tokamak, with major radius $R_0 = 1.75$ m, minor radius $a = 0.46$ m, toroidal magnetic field $B_\phi = 2.2$ T, toroidal plasma current $I_p = 350$ kA, circular cross section. The target plasmas had line averaged electron density $\bar{n}_e = 0.6 \times 10^{19}$ m^{-3}. Shafranov shift is 3 ± 1 cm. In such discharges a runaway population develops which is diagnosed by measuring the synchrotron emission with an infrared camera viewing the plasma tangentially, in the direction of electron approach (see Fig. 1). The measuring technique is described in Refs. [7–9].

In these discharges, both the primary generation (electrons in the tail of the velocity distribution crossing the critical runaway energy) and secondary generation processes (in which an already existing runaway kicks a thermal electron across the critical runaway energy [10]) are important. The latter process results in an exponential growth of the population, as witnessed by the infrared signal (Fig. 1) [11], and is independent of the plasma density.

The balance between the energy gain from the toroidal electric field and the energy loss through synchrotron radiation is reached at ~ 30 MeV [9]. Monte Carlo simulations, including the magnetic field ripple, showed that the velocity distribution develops a broad peak near this energy. The synchrotron emission is a strong function of the runaway energy [8], $\sim \gamma^2 \theta^2$ with γ the relativistic parameter and measure of energy and $\theta \equiv p_\perp / p_\parallel$ the runaway pitch angle, so that the infrared signal is dominated by the most energetic electrons in the distribution.

In the experiments described in this paper, additional plasma heating is applied using NBI, with power levels up to 0.6 MW. The Ohmic dissipation in the target plasma is ~ 0.4 MW. The NBI is switched on at $t = 3$ s, for an interval of 1.5 s. For comparison, the energy confinement time of the target plasma is $\tau_E \approx 20$ ms, the global current diffusion time $\tau_c \approx 300$ ms. Upon switching on the NBI, $\bar{n}_e$ increases. This is an unwanted effect in the present experiment, which will be discussed later.

In the Ohmic phase the runaway confinement time (τ_r) is excellent, $\tau_r > 3.5$ s [7], and the infrared signal shows an exponential rise. During the NBI interval, the infrared signals start to decrease, with a rate depending on the NBI power. Typical traces are shown in Fig. 2.

Note that, especially for the lower power levels, the signals continue to rise for up to 1 s, before the decay starts.
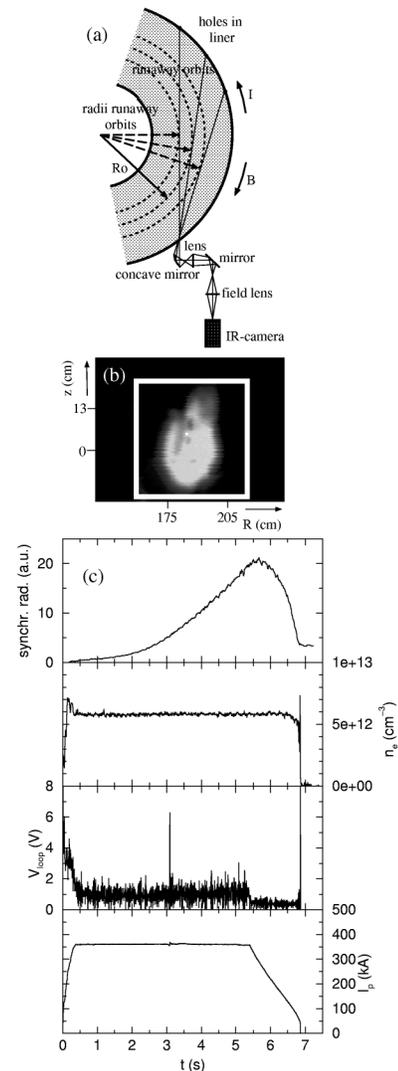

FIG. 1. (a) Setup for detection of runaway electrons in TEXTOR-94. (b) Typical IR picture showing the synchrotron radiation in a poloidal projection. Indicated is a software defined integration box. The evolution of the synchrotron radiation follows from the intergrated signal within this box. Thermal background is subtracted. (c) Time evolution of synchrotron radiation, line averaged density, loop voltage, and plasma current in an Ohmic runaway discharge.

It is this continued rise for which a physical mechanism must be found.

To interpret these signals, a simulation code has been used which calculates the synchrotron emission, taking into account the primary and secondary generation, the evolution of the runaway population in velocity space, and the diffusion in real space.

First, the effects of (i) a change of the runaway diffusion coefficient and (ii) a change of the toroidal electric field as a result of NBI (due either to heating or to current drive) were investigated. Also the combination of (i) and (ii) was studied. It was found that, while these mechanisms do lead to a decay of the synchrotron emission, the response is immediate. The continued growth of the signal could not be reproduced.
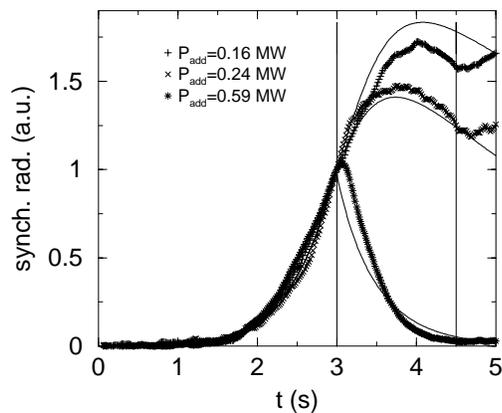
3607

FIG. 2. Measured radiation evolutions of runaway discharges (symbols) and simulated radiation evolutions (lines). Simulations have been made by application of the model of Mynick and Strachan [5] (see text). At $t = 3$ s, NBI is applied for 1.5 s, as indicated by the vertical lines. The current flat top ends at about $t = 5$ s. The curves are normalized at their synchrotron level at $t = 3$ s.

FIG. 3. Simulated radiation signals where at $t = 3$ s the confinement time of runaways changes from 5 to 0.1 s for runaways with $W < W_{loss}$. The curve for $W_{loss} = 0$ MeV is similar to the curve for the case where all newly created runaways are immediately lost.

Second, the possible increase of $\bar{n}_e$ is considered. Since the signals are well into the domain where secondary generation dominates, an increase of $\bar{n}_e$ does not affect the generation rate. Experiments were carried out in which gas puffs were applied to a target plasma without additional heating, to study the effect of the density increase alone. In those experiments the $\bar{n}_e$ increase was typically 200%. The central density increases to a similar extent as $\bar{n}_e$. It was found that the gas puff did result in a rollover of the IR signals, with delay times of 0.6 to more than 1.5 s. In comparison, for the NBI discharges presented here, the increase of $\bar{n}_e$ is negligible for <0.2 MW NBI, about 70% for 0.4 MW, increasing to 100% at 0.6 MW. We conclude that the contribution of the $\bar{n}_e$ increase to the rollover of the signals is small. Finally, since an increase of $\bar{n}_e$ does not affect the runaway generation, its effect on the IR signal must be ascribed to a deterioration of runaway confinement. It can therefore be treated on the same footing as the application of NBI power.

As a third possibility, an energy dependent change of runaway confinement was investigated, along the lines set out in the introduction. Simulations were performed in which it was assumed that, before NBI, $\tau_r = 5$ s independent of the electron energy, whereas during NBI $\tau_r = 0.1$ s for $W < W_{loss}$ and $\tau_r = 5$ s for $W \geq W_{loss}$, where W is the energy of the runaway electron. Typical results are given in Fig. 3, showing that this energy dependence does produce signal shapes very similar to those observed in the experiment.

From these simulations we conclude that, of the various mechanisms that were considered, an energy dependent runaway confinement can qualitatively reproduce the observations. This constitutes the strongest experimental proof of an energy dependent runaway confinement such as might be expected due to the averaging effect of the orbit shift.
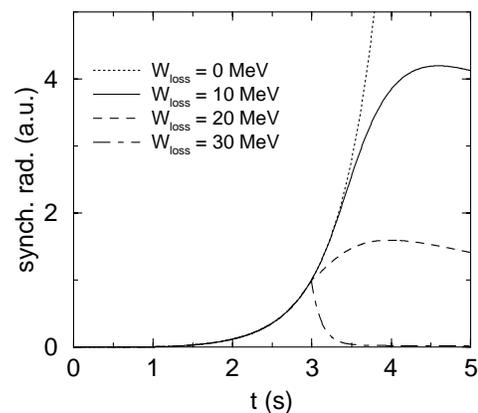
There is a degree of arbitrariness in the choice of τ_r below W_{loss}. Further, the step function is only the simplest choice to test the viability of the concept, and has no physical justification. Nonetheless, the result is fairly robust: to achieve delay times that are in the range from 1 s (which is approximately the time a 100 keV electron needs to be accelerated to the "visible" 30 MeV) down to 0.1 s or less, clearly the loss energy must vary in the range 100 keV to 30 MeV. The orbit shifts corresponding to these energies are 0.02–6 cm. For comparison, other typical scale lengths are the ion Larmor radius of approximately 0.4 cm and the inertial skin depth of about 0.2 cm. When the measured heat diffusivity in TEXTOR-94 is interpreted as a result of a random walk, a step size of 0.1 cm is estimated per transit of the torus.

To estimate the grain size of the magnetic turbulence, a further analysis has been made by adopting the theory of transport reduction due to orbit shift averaging by Mynick and Strachan [5]. This gives a prescription of the runaway confinement as a function of energy, determined by two parameters: (a) the width δ of the magnetic mode and (b) the background transport, i.e., the confinement of runaway electrons at an energy at which no transport reduction occurs. Further, the discharge parameters R_0, B_ϕ, and I_p are used to evaluate the absolute value of the orbit shift d_r according to $d_r(W) = qW/(eB_\phi c)$ with q the average safety factor. The energy dependent reduction of confinement, presented in a graph in [5], is represented by the expression

$$\frac{\tau_r}{\tau_{r,0}} \approx \left(1 + 1.1 \frac{d_r}{\delta}\right)^{5.7}$$

in the present simulations. Simulations are made in which the mode width δ is a control parameter, which is systematically varied between simulations. The reduction curve is calibrated in absolute sense by equating the test particle transport at low energy ($\tau_{r,0}$) to thermal confinement, with a correction factor for velocity, as prescribed in [5].

With the theoretical expression for the energy dependent confinement reduction, signals are obtained that are similar to the observed ones, as shown in Fig. 2. From a comparison of the simulated and measured signals, the free parameter δ, i.e., the width of the perturbing modes, is found for the different NBI power levels used in the experiment. The result is given in Fig. 4.

The figure shows that δ is an increasing function of the NBI power. The absolute values depend on the calibration of the reduction curve, which is rather uncertain. However, since the reduction curve is very steep, the absolute calibration is not a sensitive parameter; varying it by an order of magnitude changes the resulting value of δ by only a factor 2.

The values are quite similar to measurements of the radial correlation length of density fluctuations measured with correlation reflectometry in JET [12].

To estimate the contribution to thermal transport, both the level and the correlation lengths of the perturbing field must be known. In the absence of a measurement of the latter, some model must be adopted. In [13], the excursion of field lines in a realistic tokamak configuration is computed as function of the perturbing field. Equating the average excursion (which levels off after some ten toroidal transits) to the mode width, we find (following [13]) a level $\tilde{B}/B < 5 \times 10^{-5}$ for the Ohmic plasma, increasing to 10^{-3} for 0.6 MW NBI. This compares well with the values of $\tilde{B}/B$ measured in Tore Supra [2,3]. The corresponding thermal diffusivity is negligible in the Ohmic plasma, but reaches the measured diffusivity (~ 1 m^2 s^{-1}) for the highest heating power. While this is a coarse estimate, the conclusion seems justified that magnetic turbulence does not contribute to anomalous transport in the Ohmic plasma, but could become important or even dominant at high heating power.

This conclusion may also explain the observation that in the present data set the energy confinement does not deteriorate for increasing δ. For low heating power, magnetic turbulence is not the dominant loss mechanism. Moreover, with heating the density increases, which in low density plasmas leads to improved confinement, possibly through suppression of electrostatic turbulence. The runaway electrons are not sensitive to this transport mechanism, and therefore show a confinement scaling different from the thermal plasma.

In conclusion, we have shown that upon application of NBI the population of 30-MeV runaway electrons in TEXTOR-94 decays, but that this decay starts only after a delay of up to 1 s. Simulations show that an energy dependent runaway confinement can account for this delay. The delay times are associated with loss energies below which the increased runaway loss sets in. Electrons at these energies have an orbit shift of typically 0.02−6 cm.
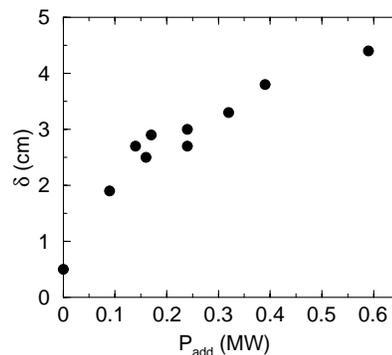

FIG. 4. Relation between averaged mode width δ and additional heating power P_{add} derived from a comparison between simulated and measured radiation signals.

By application of the theory for orbit shift suppression of runaway transport in the presence of magnetic turbulence, it was found that the perturbing magnetic modes have a typical mode width of <0.5 cm in Ohmic discharges, increasing to several cm at 0.6 MW NBI.

[1] C. M. Greenfield *et al.,* Phys. Plasmas **4**, 1596 (1997); E. Mazzucato *et al.,* Phys. Rev. Lett. **77**, 3145 (1996).
[2] X. L. Zou *et al.,* Phys. Rev. Lett. **75**, 1090 (1995).
[3] L. Colas *et al.,* Nucl. Fusion **38**, 903 (1998).
[4] J. D. Strachan, Nucl. Fusion **16**, 743 (1976); C. W. Barnes, J. M. Stavely, and J. D. Strachan, Nucl. Fusion **21**, 1469 (1981); C. W. Barnes and J. D. Strachan, Phys. Fluids **26**, 2668 (1983); S. J. Zweben, D. W. Swain, and H. H. Fleischmann, Nucl. Fusion **18**, 1679 (1978); P. J. Catto *et al.,* Phys. Fluids B **3**, 2038 (1991); J. R. Myra *et al.,* Phys. Fluids B **4**, 2092 (1992); O. J. Kwon *et al.,* Nucl. Fusion **28**, 1931 (1988).
[5] H. E. Mynick and J. D. Strachan, Phys. Fluids **24**, 695 (1981).
[6] R. Jaspers *et al.,* Phys. Rev. Lett. **72**, 4093 (1994).
[7] I. Entrop, N. J. Lopes Cardozo, R. Jaspers, and K. H. Finken, Plasma Phys. Controlled Fusion **40**, 1513 (1998).
[8] K. H. Finken *et al.,* Nucl. Fusion **30**, 859 (1990).
[9] R. Jaspers, Ph.D. thesis, Eindhoven University of Technology, The Netherlands, 1995.
[10] N. T. Besedin and I. M. Pankratov, Nucl. Fusion **26**, 807 (1986).
[11] R. Jaspers *et al.,* Nucl. Fusion **33**, 1775 (1993).
[12] A. E. Costley, P. Cripwell, and T. Fukuda, in *Proceedings of the 21st EPS Conference on Controlled Fusion and Plasma Physics, Innsbruck, 1994* (EPS, Innsbruck, 1994), Part I, p. 199.
[13] M. de Rover, A. M. R. Schilham, A. Montvai, and N. J. Lopes Cardozo, Phys. Plasmas **6**, 2443 (1999).